Original Article

Boundary effect of toppling failure based on three-dimensional mechanical model

CAI Jun-chao[1,2,3] https://orcid.org/0000-0002-7152-5803; e-mail: caijunchaocdut@126.com

ZHENG Da[2,3]* http://orcid.org/0000-0003-1640-7190; ✉e-mail: zhengda@cdut.cn

JU Neng-pan[2,3]* http://orcid.org/0000-0002-3159-1689; ✉e-mail: jnp@cdut.edu.cn

HUANG Run-qiu[2,3] http://orcid.org/0000-0003-2560-4962; e-mail: hrq@cdut.edu.cn

ZHAO Wei-hua[2,3] http://orcid.org/0000-0003-3010-1841; e-mail:weihuageo@gmail.com

*Corresponding author

1 School of Civil Engineering, Henan University of Science and Technology, Luoyang 471023, China

2 State Key Laboratory of Geohazard Prevention and Geoenvironment Protection, Chengdu University of Technology, Chengdu 610059, China

3 College of Environment and Civil Engineering, Chengdu University of Technology, Chengdu 610059, China

Abstract: Previous researches on the mechanical model of toppling failure mainly concentrated on two-dimensional mechanical model (TwDM) analysis. The TwDM analysis assumes the width of the slab beam is unit width without considering the lateral constraint force. The assumed conditions are obviously different from the site conditions, thus there is a certain difference between the calculated results and the field work. A three-dimensional mechanical model (ThDM) of toppling failure was established, considering that the slab beam was mainly subject to self-weight, the frictional resistance of interlayer and lateral constraint force. Due to the progressive characteristics of toppling failure, the concept and the formula of the first fracture depth (FFD) of toppling was raised and constructed. The case study indicates that the ThDM is more effective and can be accurately used to calculate the toppling fracture depth of the slab beam. The FFD decreases proportionally with the increase of slab beam width. FFD grows fast when the slab beam width is less than 2.0 m and it tends to be stable when the slab beam width is above 2.0 m. The FFD decreases with the increase of the lateral constraint coefficient, indicating that the boundary condition of the free space is positively correlated with the stability and depth of toppling. This is a good explanation of the free space effect. This study provides a reference for the stability evaluation and prevention-control design of toppling slope in the future.

Keywords: Boundary effect; Toppling failure; Three-dimensional mechanical model (ThDM); First fracture depth (FFD); Free face; Slope failure

1 Introduction

Toppling failure, as a typical slope failure, has

been reported in more and more situations with the constructions of mines, highways, hydropower stations and so on (DeFreitas and Watters 1973; Wyllie 1980; Aydan and Kawamoto 1992; Cruden and Hu 1994; Tamrakar et al. 2002; Huang 2007; Liu et al. 2016; Zhang et al. 2018; Zhu et al. 2022). Goodman summarized the developments in the research on toppling deformation and concluded that toppling generally occurs in foundations, tunnels and underground chambers, or on a small scale in any rocky landscape where frost, creep, or water forces are active (Goodman 2013).

Based on the long-term observation of the toppling deformation phenomenon, it has been proposed that the degree of the deformation and failure of toppling will be more intense with better open space conditions (or the conditions of free face). As shown in Fig. 1, the toppling bank slope of hydropower station in Qinghai province, Northwest China, is obviously developed in the protruding part of the ridge and weak in the edge of the gully (Cai et al. 2019).

The same phenomenon appears on the bank slope of Miaowei hydropower station on Lancang river. The development situation, which was shown in Fig. 2, presented the boundary effect of toppling deformation. It is worth noting that the toppling deformation is distinguished in different space boundary. Previous studies focused on the influence factors of toppling, the two-dimensional mechanical model of that and the development process and formation mechanism of toppling (Huang et al. 2017; Alejano et al. 2018; Zheng et al. 2018; Ning et al. 2019; Zhu et al. 2020; Tao et al. 2021; Zhang et al. 2022). The method of Goodman and Bray (GB method) was

firstly proposed by Goodman and Bray to analyze toppling, focusing on the toppling stability of known basal plane and the shallow toppling (Goodman and Bray 1976). However, the basal plane of deep toppling is unknown. On this basis, a cantilever beam model is proposed. Domestic and foreign scholars have carried out various studies on the application of the cantilever beam theory for toppling. The cantilever beam theory was presented by Sun et al. to study the slab fracture rock mass (Sun and Zhang 1985; Sun 1988). Aydan et al. (1992) and Adhikary et al. (1997, 2007) established a cantilever beam toppling model based on the limit equilibrium theory, and assumed that the interaction force between layers is a concentrated force, only considering the self-weight of the rock layer, which was verified in later experiments (Aydan and Kawamoto 1992; Adhikary et al. 1997; Adhikary and Dyskin 2007). A cantilever beam model, presented by Chen and Huang (2004), regarded the rock layer as the instantaneous free-space state of the lower part, considering only the self-weight of the rock layer and the additional load of the upper rock slabs. Jiang and Huang (2006) generalized the rocky strata into an elastic plate beam model with a fixed lower end and a free upper end. Considering the self-weight and the interlayer dislocation resistance of the slab beam, it was assumed that the normal interlayer stress was a triangular distribution. Amini et al. (2009, 2012) combined the GB method with the method of Aydan to introduce a solution for the analysis of block-flexure toppling failure, and proposed an efficient method for analysis of the toppling based on compatibility principles governing the behavior of cantilever beams. Later, Amini et al. (2017, 2018) analyzed a slide-toe-toppling failure and a slide-head-
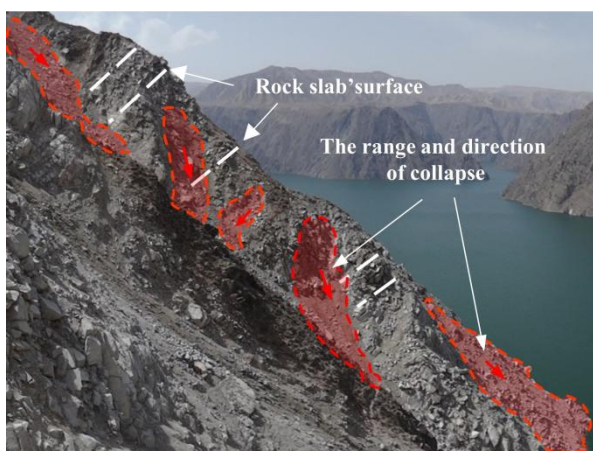
Fig. 1 Toppling at mid-lower ridge #3 of bank slope of hydropower station.

Fig. 2 Toppled rock mass of the highway slope at Miaowei hydropower station.

toppling failure with that method. Cai et al. (2014) simplified the rocky strata into a cantilever beam, considering the self-weight of the slab beam and the interlayer friction resistance. The normal stress between layers was distributed in an irregular shape. Based on the progressive failure characteristics of ductile flexural toppling failure, Cai et al. (2022) used two-dimensional mechanics to analyze its time-varying effect, and discussed the development conditions of start-up, transient stability and long-term creep development stages respectively. The above researches are based on two-dimensional mechanical model (TwDM) analysis, without considering the lateral constraint force and the width variation. The TwDM with width of 1.0 m indicates that the lateral joint spacing is the unit width, but lateral spacing is generally w≠1.0 m. The boundary effect was neglected and herein the three-dimensional mechanical model (ThDM) was seldom built. The purpose of this study is to establish a ThDM of toppling, and to illustrate the boundary effect of the toppling caused by lateral constraint. The lateral constraint coefficient was drawn to reflect the lateral constraint conditions.

Existing models researched by Brideau and Stead (2010) also reflected the effect of boundaries on toppling failure, which presents the characteristics of deformation and failure of block toppling caused by different constraints. Fig. 3 demonstrates that the toppling failure model without lateral constraints on the right and that with lateral constraints on the left. The development depth and scope of the toppl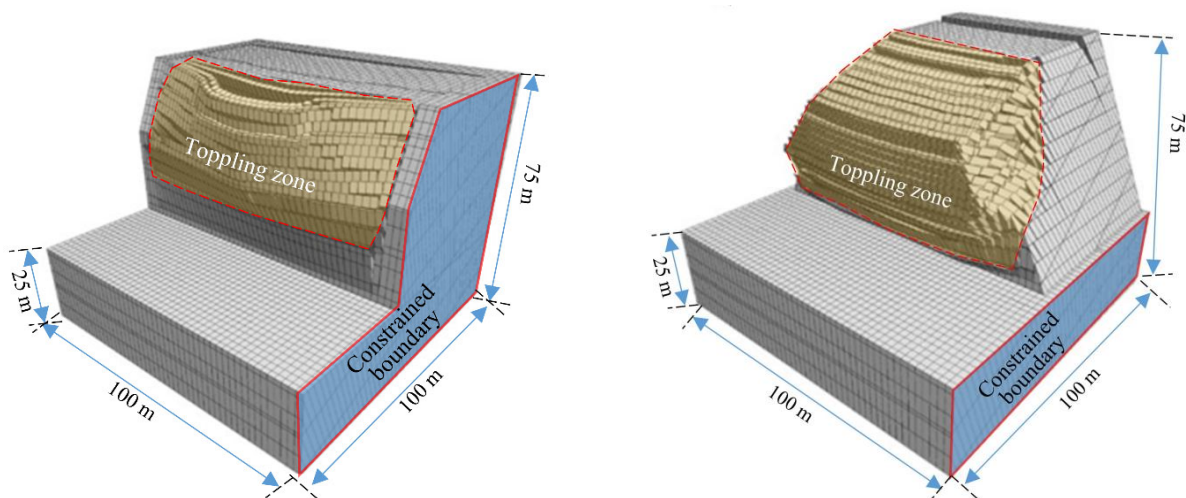ing failure model without lateral constraints are considerable, and the boundary effect of toppling failure is brightly depicted in Fig. 3.

In this study, we investigated the boundary effect of the toppled slope with mechanics analysis. A three-dimensional mechanical model (ThDM) was established to further discuss the impact of different boundary conditions. The parameter analysis and application case of toppling failure were applied to verify the mechanical analysis and to explain the field geological phenomenon. In addition, it provided robust evidence for future protection. To improve the stability of the engineering slope, systematic support should be set at appropriate positions according to local conditions, or the deformation body should be removed to proper depth by excavation. Besides, it can be used for the further analysis and evaluation of the suitability of the engineering.

2 Mechanical Model and Assumption

In this study, the cantilever beam theory was applied to establish a three-dimensional mechanical model (ThDM). A ThDM was established for a single slab beam, which is summarized to solve the problem, considering the action of self-weight, interlaminar friction resistance, and lateral constraining force on the slab beam (Fig. 4).

The following assumptions were made to simplify the analysis. (1) The slab beam is always in a quasi-equilibrium state during the process of bending and toppling, and is subject to self-weight, the friction resistance of the upper and lower adjacent layers and

Fig. 3 Toppling failure models, after Brideau and Stead (2010). Left: lateral boundary constrained model. Right: lateral boundary unconstrained model.
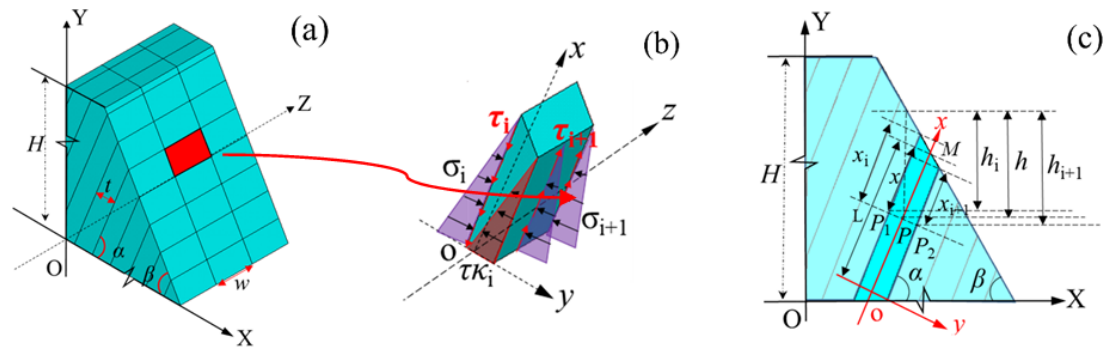
Fig. 4 Geometry of the mechanical model. (a) Three-dimensional mechanical model; (b) A single slab beam; (c) Side view of model.

lateral constraining force of the left and right sides. (2) The stress at a certain point in the rock mass can be simplified as the vertical self-weight stress and the horizontal lateral stress. (3) The rock layer is homogeneous and uniform in thickness, and the distribution of normal stress and shear stress between layers and lateral joints is linear, and only related to the buried depth. Besides, the cohesion and internal frictional angle of the strata are the same, and that of the lateral joints are also uniform. It is assumed that the parameters of joint surface are equal to those of the stratum plane. Meanwhile, considering that the joint surface is almost open after unloading, and the cohesion of the joint surface is limited, the influence of the cohesion of the lateral joint surface is not considered in this study.

3   Mechanical Analysis of Toppling Failure

Fig. 4 presents the mechanical model under the global coordinate system, H—the height of slope, α— the dip angle of the strata ($0 < \alpha < 90°$); β— the angle of the slope ($0 < \beta < 90°$); t — the thickness of the single-layer slab beam; w — the width of the slab beam; L — the length from the fracture surface to the slope surface. A certain rock slab was selected as the research object established at the local coordinate system (Fig. 4b). The extension direction of the bedding plane was the x-axis, the vertical direction of the bedding plane was the y-axis, and the width direction of the slab beam was the z-axis. O is the fixed end, OM is the cantilever segment of the rock slab, P is any point on the slab beam. x is the length along the bedding direction of point P to the slope surface, h is the vertical depth of point P from this point to the slope surface in the vertical direction, and

h_i and h_{i+1} are the vertical depths of P_1 and P_2, respectively. According to the geometric relationship of the model, the vertical depths of points P, P_1 and P_2 were expressed as Eq. (1).

$$h = x \sin(\alpha + \beta) / \cos \beta$$

$$h_i = x \sin(\alpha + \beta) / \cos \beta - t \cos(\alpha + \beta) / 2\cos \beta \qquad (1)$$

$$h_{i+1} = x \sin(\alpha + \beta) / \cos \beta + t \cos(\alpha + \beta) / 2\cos \beta$$

3.1 Interlayer friction

The self-weight stresses at P_1 and P_2 are $\sigma_{vi} = \gamma h_i$ and $\sigma_{v(i+1)} = \gamma h_{(i+1)}$ respectively, and the horizontal lateral stress are $\sigma_{hi} = n\gamma h_i$ and $\sigma_{h(i+1)} = n\gamma h_{(i+1)}$. Where, n is the lateral stress coefficient, and its calculation formula is:

$$n = \mu/(1 - \mu) \qquad (2)$$

where, μ is Poisson's ratio.

According to the principle of rock mechanics, it is presumed that the slab beam is under the conditions of self-weight, horizontal stress, z-direction of horizontal lateral constraint, and the lateral constraints of friction between the joint surface and the slab beams. Because the lateral constraint is vertical to the lateral section, the slab beam can be selected as the research object of the mechanical analysis, and then simplified as a two-dimensional plane stress model and the lateral constraint force for analysis. The stress of the slab beam is decomposed into the normal stress and the shear stress. A micro-element is selected in the slab beam, and a certain oblique section of the micro-element is taken to form an angle θ from the large principal stress surface, as shown in Fig. 5. According to the balance conditions of the force, the following relations are obtained.
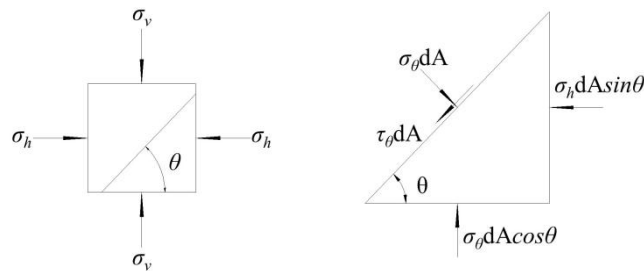
Fig. 5 Micro-element and cross-section stress state of the slab beam.

$$\sigma_\theta = \frac{\sigma_v + \sigma_h}{2} + \frac{\sigma_v - \sigma_h}{2} \cos 2\theta$$
$$\tau_\theta = \frac{\sigma_v - \sigma_h}{2} \sin 2\theta \qquad (3)$$

Because of $n\sigma_v = \sigma_h$, the stress state at a point in

$$\sigma_i = \gamma h_i \lambda$$
$$\sigma_{i+1} = \gamma h_{i+1} \lambda$$
$$\tau_i = tan\varphi\gamma h_i \lambda + c \qquad (5)$$
$$\tau_{i+1} = tan\varphi\gamma h_{i+1} \lambda + c$$

the slab beam is as follows:

$$\sigma_\alpha = \gamma h\left[\frac{1+n}{2} + \frac{1-n}{2} \cos 2\alpha\right]$$
$$\tau_\alpha = \gamma h \frac{1-n}{2} \sin 2\alpha \qquad (4)$$

Because the toppling is still in the quasi-static equilibrium of dislocation each other and meets $\tau_i > [\tau] = \sigma \tan \varphi + c$, the rock slab can slide along the plane of rock layer. Thus, $\lambda = \frac{1+n}{2} + \frac{1-n}{2} \cos 2\alpha$, Eq. (4) can be rewritten as follows.

3.2 Lateral constraint force

The lateral constraint force of the lateral section can be decomposed into normal stress and shear stress on the joint surface, which meet the dislocation conditions. Namely, $\sigma k_i = n\gamma h_i$, $\tau k_i > [\tau] = \sigma \tan \varphi + c$.

The introduced lateral constraint coefficient K presented lateral constraint conditions, which reflected the boundary condition of the slab beam. Supposing $K \in [0, 2]$, 0 means no constraint, which reflects the three-way conditions of free face. 1 shows a unilateral constraint that reflects the condition on either side of the free face. 2 signifies three constraints and only one side opening condition. The values of (0, 1) or (1, 2) correspond to different combinations of opening conditions, considering unloading crack conditions (including two free faces,

unloading conditions and one free face). Those values are determined according to the opening and filling degree of unloading cracks. Due to the limited contribution of cohesion after opening, only the friction angle effect is taken into consideration. We obtain

$$\sigma k_i = n\gamma h_i$$
$$\tau k_i = Ktan\varphi n\gamma h_i \qquad (6)$$

3.3 Toppling failure criterion

According to the force analysis of the above three-dimensional geomechanical model, the length of the slab beam is x. The thickness is t, and the width is w. σ_{n1} and σ_{n2} are the normal stresses of the slab beam, respectively. τ_1 and τ_2 are respectively the shear stresses of the slab beam surface, and τk_i is the lateral constraint force. W is the self-weight of the slab beam. Therefore, $W = \gamma txw$. M, the difference between the bending moment M_T and the resisting moment M_R, is the total bending moment of the slab beam. M can be abbreviated as follows:

$$M = M_T - M_R = -\frac{1}{4}\gamma x^2 tw\lambda \frac{cos(\alpha+\beta)}{cos\beta}$$
$$-\frac{1}{2}\gamma x^2 twtan\varphi\lambda \frac{sin(\alpha + \beta)}{cos \beta} + \frac{1}{2}\gamma x^2 twcos\alpha \qquad (7)$$
$$-cxtw + \frac{1}{12}tx^3 \frac{sin(\alpha + \beta)}{cos\beta} Kn\gamma tan\varphi$$

Since the compressive strength of the rock mass is much higher than its tensile strength, tensile failure is likely to occur. In other words, the condition of toppling failure of the slab beam is $M > 0$ and $\sigma_t > [\sigma_T]$. σ_t and $[\sigma_T]$ are the tensile stress of the slab beam and the tensile strength of the rock mass, respectively. The tensile stress on the normal section of the beam can be expressed as:

$$\sigma_t = \frac{My}{I} - \frac{N}{A} + w\int_0^x \frac{\tau_{i+1} - \tau_i}{tw} dx =$$

$$\frac{-\frac{3}{2}\gamma x^2 \lambda \frac{cos(\alpha+\beta)}{2cos\beta}-3\gamma x^2 tan\varphi\lambda\frac{sin(\alpha+\beta)}{cos\beta}+3\gamma x^2 cos\alpha-6cx}{t}+$$

$$\frac{\frac{1}{2}x^3\frac{sin(\alpha+\beta)}{cos\beta}Kn\gamma tan\varphi}{tw}-\gamma x sin\alpha \qquad (8)$$

where, N is the axial force exerted on the slab beam, which is the component force of the self-weight of the slab beam in the x-direction, $N = W sin\alpha$. A is the normal cross-sectional area of the slab beam, $A = tw$. y is the distance in the y-direction from the fracture point on the normal section to the centroid of the section, $y = t/2$. I is the section moment of inertia, $I = t^3w/12$.

$$A_1 = \frac{\frac{sin(\alpha+\beta)}{cos\beta}Kn\gamma tan\varphi}{2tw} \qquad (9)$$

$$B_1 = \frac{-\frac{3}{2}\gamma\lambda\frac{cos(\alpha+\beta)}{2cos\beta}-3\gamma tan\varphi\lambda\frac{sin(\alpha+\beta)}{cos\beta}+3\gamma cos\alpha}{t} \qquad 10)$$

$$C_1 = \frac{-6c}{t} + \gamma\,tan\,\varphi\,\lambda\frac{cos(\alpha+\beta)}{cos\beta} - \gamma sin\alpha \qquad (11)$$

$$D_1 = -[\sigma_T] \qquad (12)$$

$$A_1 x^3 + B_1 x^2 + C_1 x + D_1 = 0 \qquad (13)$$

According to Cardin's formula, if $A_1 \neq 0$, there must be a real solution of the unary cubic equation, A_1, B_1, C_1, $D_1 \in R$. Moreover, the solution is the first toppling fracture depth of the slab beam.

$$A_0 = -\frac{B_1}{3A_1} \qquad (14)$$

$$B_0 = -\frac{27A_1 2D_1 - 9A_1 B_1 C_1 + 2B_1 3}{54A_1 3} \qquad (15)$$

$$C_0 = \sqrt{\left(\frac{27A_1^2 D_1 - 9A_1 B_1 C_1 + 2B_1^3}{54A_1^3}\right)^2 + \left(\frac{3A_1 C_1 - B_1^2}{9A_1^2}\right)^3} \qquad (16)$$

According to Cardin's formula, the first fracture depth x of the slab beam is:

$$x = A_0 + \sqrt[3]{B_0 + C_0} + \sqrt[3]{B_0 - C_0} \qquad (17)$$

If $A_1 = 0$, Eq. (13) is simplified to a unary quadratic equation, namely, $B_1 x^2 + C_1 x + D_1 = 0$, the first fracture depth x of the slab beam is as follows:

$$x = \frac{-C_1 + \sqrt{C_1^2 - 4B_1 D_1}}{2B_1} \qquad (18)$$

It is consistent with the format of the previous two-dimensional mechanical model of the slab beam and will not be described in detail. From Eq. (17), it can be inferred that the first toppling fracture depth of the slab beam is closely related to slope angle β, rock inclination angle α, the weight of the slab beam γ, thickness t, width w, lateral constraint coefficient n, internal friction angle of the rock layer φ, cohesion of the rock layer c, and lateral constraint factor K. The following variable analysis was further analyzed the boundary effect of toppling.

4 Variable Analysis

4.1 Application case

The toppling slope of the highway, proposed by Liu et al. (2016), in the southern mountainous area of Anhui was taken as an example. The slope lithology is composed of metamorphic sand slate, and the inclination angle of the rock layer α = 56°, the slope angle β = 50°, γ= 26.0 kN/m³, Poisson's ratio μ = 0.2, t = 0.25 m, the tensile strength $[\sigma_T]$ = 9 000 kPa, φ = 20°, c = 50 kPa. The coefficient of lateral stress n = 0.25 can be obtained from Eq. (2). According to the K values of (0, 1) or (1, 2) correspond to different combinations of opening conditions, considering including two free faces or unloading conditions and one free face. This site point is located in the mountain ridge, and the slope side is a gully on one side and an excavation surface of the highway on the other side. This site point approximately presented two free faces, then w =2.0 m, and the coefficient of lateral constraint K=0.01 can be determined according to the geological conditions in the field (Table 1). According to Eq. (17), the toppling fracture depth of ThDM is 14.7 m. The depth calculated by the TwDM is 14.0 m, and the toppling development depth measured in the field is about 15.5 m.

The slope angle β, rock inclination angle α, the weight of the slab beam γ, thickness t, width w, lateral constraint coefficient n, internal friction angle of the rock layer φ, cohesion of the rock layer c can obtain from field geological surveys and mechanical tests. The coefficient of lateral constraint K can be determined by referring to Table 1.

Obviously, Eq. (17) derived from the ThDM can be used to accurately calculate the toppling fracture depth of the slab beam, and the results are consistent with the depth of the statistical field. The difference between the calculated depth and the measured depth can be attributed to the following three reasons. Firstly, in the mechanical model analysis, the stress state of the slope is simplified without considering the geological and environmental factors such as the tectonic stress and the unique structure of the slope. Secondly, field statistics of the fracture depth by geologists are not the first toppling fracture depth, but generally the final depth of multiple toppling and bending fracture. Finally, it is difficult to measure the fragmentized rock mass in the toppling fracture zone, which is also the reason for the difference.

Table 1 Description of the situation for determining the value of K

Coefficient of lateral constraint K	Description of the situation	Diagram of the situation
0	0 means no constraint, which reflects the three-way conditions of free face, D01.	
0-1	(0-1) correspond to different combinations of opening conditions, considering unloading crack conditions, including two free faces or unloading conditions and one free face.	
1	A unilateral constraint that reflects the condition on either side of the free face, D03 and D05.	
1-2	(1-2) correspond to different combinations of opening conditions, considering unloading crack conditions, including two free faces or unloading conditions and one free face.	
2	2 signifies three constraints and only one side opening condition, D02 and D04.	
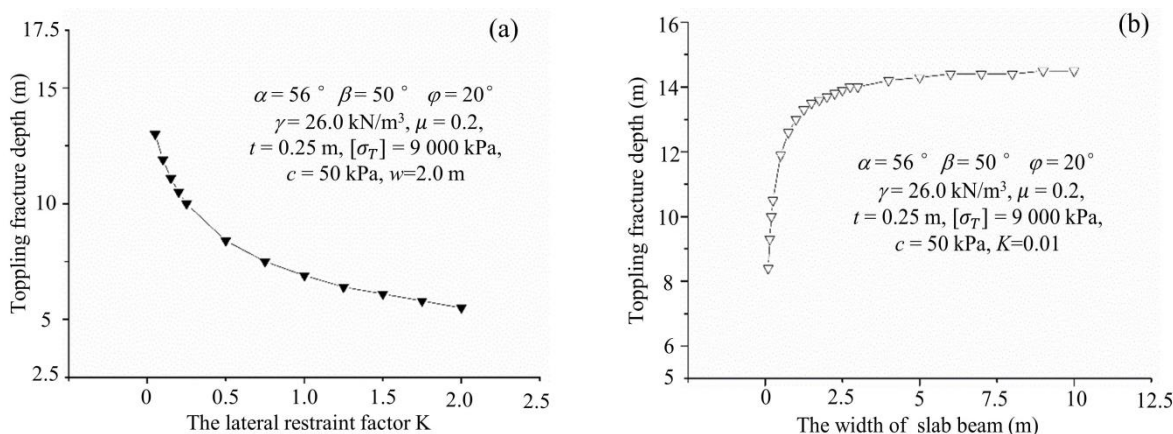
Fig. 6 Relationship between toppling fracture depth and lateral constraint coefficient and width of the slab beam.

The ThDM we established considers more factors than the TwDM, and the scope of use is wider than that of the TwDM. Since the compressive strength of the rock mass is much higher than its tensile strength, tensile failure is likely to occur. The ThDM and TwDM are mainly aimed at the brittle failure of tensile failure, and there will be certain discrepancies for ductile deformation.

4.2 Variable analysis

Taking the toppling slope of the highway investigated by Liu et al. (2016) as an example, the control variable method is supposed to study further the first toppling fracture depth of the slab beam and the related variables. The variables including the lateral constraint coefficient K and the width w of the slab beam were mainly selected, and the curves of the relationship between the variables and the first toppling fracture depth illustrated in Fig. 6 are concluded.

According to the parameter analysis (Fig. 6), the first fracture depth (FFD) of the slab beam increases with the increase of width, and decreases with the rise of lateral constraint coefficient. Thereinto the FFD increases inversely with the increase of the width of the slab beam. FFD grows fast at the early stage of $w <$ 2.0 m, and it tends to be stable when $w >$ 2.0 m. The FFD decreases with the growth of the lateral constraint coefficient of the slab beam, which indicates that under the same conditions, the better the condition of free face is, the more likely the toppling failure occurs, and the greater the toppling fracture depth.

The two-dimensional mechanical model (TwDM) with width of 1.0 m indicates that the lateral joint spacing is the unit width. In most cases, lateral spacing is generally $w \neq 1.0$ m, and there is no lateral

constraint force caused by the principal stress. Therefore, there is a difference between the measured depth and the calculation depth. The TwDM is still insufficient. The three-dimensional mechanical model (ThDM) established in this study can better reflect the stress state of the actual toppling failure of the site. Besides, it is of more practical significance to obtain the first fracture depth, and it is necessary to further study the subsequent second or multiple toppling fractures after the first toppling fracture.

5 Conclusion

Based on the progressive features of the toppling failure, the concept of the first fracture depth (FFD) of toppling is proposed.

Considering the variation of gravity, the friction resistance between layers and the lateral constraint of the slab beam along with width, a three-dimensional mechanical model (ThDM) of toppling failure is established to obtain the first fracture depth of toppling failure.

Based on the first fracture depth formula of the ThDM of toppling failure, the typical case of toppling slope is selected to verify the calculation, and the results are corresponding to the field occurrence. It presents that the ThDM can be accurately used to calculate the toppling fracture depth. Besides, considering the simplification of the model and the human factors of geologists' statistics, the field occurrence is distinguished from calculation results.

When the lateral constraint coefficient K=0, the established ThDM is simplified to a two-dimensional mechanical model (TwDM), and the solution for the first fracture depth is Eq. (18). The results show that the first fracture depth (FFD) grows fast when $w < 2.0$ m, and it tends to be stable when w is above 2.0 m. The FFD decreases with the increase of the lateral constraint coefficient, indicating that the better the condition of free face is, the more easily the toppling failure initiates, and the deeper the toppling fracture depth is. The research results explained the boundary effect of the free face well. This study provides a reference for the stability evaluation, prevention-control design and the engineering suitability of toppling slope in the future.

References

Adhikary DP, Dyskin AV, Jewell RJ (1997) A study of the mechanism of flexural toppling failure of rock slopes. Rock Mech Rock Eng 30: 75-93.
https://doi.org/10.1007/BF01020126

Adhikary DP, Dyskin AV (2007) Modelling of progressive and instantaneous failures of foliated rock slopes. Rock Mech Rock Eng 40(4): 349-362.
https://doi.org/10.1007/s00603-006-0085-8

Alejano LR, Alonso CS, Rey IP, et al. (2018) Block toppling stability in the case of rock blocks with rounded edges. Eng Geol 234: 192-203.
https://doi.org/10.1016/j.enggeo.2018.01.010

Amini M, Akbar A, Mohammad HK (2017) Stability analysis of slide-toe-toppling failure. Eng Geol 228: 82-96.
https://doi.org/10.1016/j.enggeo.2017.07.008

Amini M, Hassan S, Kamran E (2018) Stability analysis of slopes with a potential of slide-head-toppling failure. Int J Rock Mech Min 112: 108-121.
https://doi.org/10.1016/j.ijrmms.2018.09.008

Amini M, Majdi A, Aydan, Ö (2009) Stability analysis and the stabilisation of flexural toppling failure. Rock Mech Rock Eng 42: 751-782.
https://doi.org/10.1007/s00603-008-0020-2

Amini M, Majdi A, Veshadi MA (2012) Stability analysis of rock slopes against block flexure toppling failure. Rock Mech Rock Eng 45: 519-532.
https://doi.org/10.1007/s00603-012-0220-7

Aydan O, Kawamoto T (1992) The stability of slopes and underground openings against flexural toppling and their stabilization. Rock Mech Rock Eng 25: 143-165.
http://doi.org/10.1007/BF01019709

Brideau MA, Stead D (2010) Controls on block toppling using a three dimensional distinct element approach. Rock Mech Rock Eng 43: 241-260.
https://doi.org/10.1007/s00603-009-0052-2

Cai JC, Ju NP, Huang RQ, et al. (2019) Mechanism of toppling and deformation in hard rock slope: a case of bank slope of Hydropower Station, Qinghai Province, China. J Mt Sci 16: 924-934.
https://doi.org/10.1007/s11629-018-5096-x

Cai JC, Zheng D, Ju NP, et al. (2022) Time-varying effect of ductile flexural toppling failure on antidip layered rock Slope. Front Earth Sci 10:943700.
https://doi.org/10.3389/feart.2022.943700

Cai JS, Yan EC, Wang ZQ, et al. (2014) Study of cantilever beam limit equilibrium model of anti-dip layered rock slopes. Rock Soil Mech 35(S1): 15-28.
https://doi.org/10.16285/j.rsm.2014.s1.003

Chen HQ, Huang RQ (2004) Stress and flexibility criteria of bending and breaking in a countertendency layered slope. Chin J Eng Geol 12: 243-246, 273. (In Chinese)
https://doi.org/10.3969/j.issn.1004-9665.2004.03.004

Cruden DM, Hu XQ (1994) Topples on underdip slopes in the Highwood Pass, Alberta, Canada. Q J Eng Geol Hydroge 27: 57-68.
https://doi.org/10.1016/0148-9062(94)91232-7

DeFreitas MH, Watters RJ (1973) Some field examples of toppling failure. Geotechnique 23: 495-514.
http://doi.org/10.1680/geot.1973.23.4.495

Goodman RE (2013) Toppling-A fundamental failure mode in discontinuous materials Description and analysis. In: 2013 Congress on Stability and Performance of Slopes and Embankments III, Geo-Congress 2013, San Diego, United States. Geotechnical Special Publication. ASCE pp 2348-2378.
https://doi.org/10.1061/9780784412787.227

Goodman RE, Bray JW (1976) Toppling of rock slopes, in Rock Engineering for Foundations & Slopes. ASCE pp 201-234.

Huang RQ (2007) Large-scale Landslides and their sliding mechanisms in China Since the 20th Century. Chin J Rock Mech Eng 26: 433-454. (In Chinese)
https://doi.org/10.3321/j.issn:1000-6915.2007.03.001

Huang RQ, Li YS, Yan M (2017) The implication and evaluation of toppling failure in Engineering geology practice. Chin J Eng Geol 25: 1165-1181. (In Chinese)
https://doi.org/10.13544/j.cnki.jeg.2017.05.001

Jiang LW, Huang RQ (2006) Bending yielding and tensile cracking critera for failure of rock slope whose dip direction opposite to the dip direction of strata. Chin J Eng Geol 14: 289-294, 429. (In Chinese)
https://doi.org/10.3969/j.issn.1004-9665.2006.03.001.

Liu HJ, Zhao JJ, Ju NP (2016) Mechanical analysis of toppling failure of rock slope. Rock Soil Mech 37: 289-294.
https://doi.org/10.16285/j.rsm.2016.S1.038

Liu M, Liu FZ, Huang RQ, et al. (2016) Deep-seated large-scale toppling failure in metamorphic rocks: a case study of the Erguxi slope in southwest China. J Mt Sci 13: 2094-2110.
https://doi.org/10.1007/s11629-015-3803-4

Ning YB, Zhang GC, Tang HM, et al. (2019) Process analysis of toppling failure on anti dip rock slopes under seismic load in Southwest China. Rock Mech Rock Eng 52: 4439–4455.
https://doi.org/10.1007/s00603-019-01855-z

Sun GZ (1988) Structural mechanics of rock mass. Beijing: Science Press. pp 363-365. (In Chinese)

Sun GZ, Zhang WB (1985) A common rock structure-board crack structure and its mechanical model. Chin J Geol 28: 275-282. (In Chinese)

Tamrakar NK, Yokota S, Osaka O (2002) A toppled structure with sliding in the Siwalik Hills, midwestern Nepal. Eng Geol 64: 339-350.
https://doi.org/10.1016/S0013-7952(01)00095-3

Tao ZG, Zhu C, He MC, et al. (2021) A physical modeling-based study on the control mechanisms of Negative Poisson's ratio anchor cable on the stratified toppling deformation of anti-inclined slopes. Int J Rock Mech Min 138: 104632.
https://doi.org/10.1016/j.ijrmms.2021.104632

Wyllie DC (1980) Toppling rock slope failures, examples of analysis and stabilization. Rock Mechanics 13: 89-98.
http://doi.org/10.1007/BF01238952

Zhang GC, Wang F, Zhang H, et al. (2018) New stability calculation method for rock slopes subject to flexural toppling Failure. Int J Rock Mech Min 106: 319-328.
https://doi.org/10.1016/j.ijrmms.2018.04.016

Zhang P, Zhang DF, Yang Y, et al. (2022) A case study on intergrated modeling of spatial information of a complex geological body. Lithosphere 2022(s10): 2918401.
https://doi.org/10.2113/2022/2918401

Zheng Y, Chen CX, Liu TT, et al. (2018) Study on the mechanisms of flexural toppling failure in anti-inclined rock slopes using numerical and limit equilibrium models. Eng Geol 237: 116-128.
https://doi.org/10.1016/j.enggeo.2018.02.006

Zhu C, He MC, Karakus M, et al. (2020) Investigating toppling failure mechanism of anti-dip layered slope due to excavation by physical modelling. Rock Mech Rock Eng 53(11): 5029-5050.
https://doi.org/10.1007/s00603-020-02207-y

Zhu C, Karakus M, He MC, et al. (2022) Volumetric deformation and damage evolution of Tibet interbedded skarn under multistage constant-amplitude-cyclic loading. Int J Rock Mech Min 152: 105066.
https://doi.org/10.1016/j.ijrmms.2022.105066